Functional ryanodine receptors in the membranes of neurohypophysial secretory granules

James M. McNally,[1,2] Edward E. Custer,[1,2] Sonia Ortiz-Miranda,[1,2] Dixon J. Woodbury,[3] Susan D. Kraner,[4] Brian M. Salzberg,[4,5] and José R. Lemos[1,2]

[1]Department of Microbiology and Physiological Systems and [2]Program in Neuroscience, University of Massachusetts Medical School, Worcester, MA 01655

[3]Department of Physiology and Developmental Biology, Brigham Young University, Provo, UT 84602

[4]Department of Neuroscience and [5]Department of Physiology, Perelman School of Medicine at the University of Pennsylvania, Philadelphia, PA 19104

Highly localized Ca^{2+} release events have been characterized in several neuronal preparations. In mouse neurohypophysial terminals (NHTs), such events, called Ca^{2+} syntillas, appear to emanate from a ryanodine-sensitive intracellular Ca^{2+} pool. Traditional sources of intracellular Ca^{2+} appear to be lacking in NHTs. Thus, we have tested the hypothesis that large dense core vesicles (LDCVs), which contain a substantial amount of calcium, represent the source of these syntillas. Here, using fluorescence immunolabeling and immunogold-labeled electron micrographs of NHTs, we show that type 2 ryanodine receptors (RyRs) are localized specifically to LDCVs. Furthermore, a large conductance nonspecific cation channel, which was identified previously in the vesicle membrane and has biophysical properties similar to that of an RyR, is pharmacologically affected in a manner characteristic of an RyR: it is activated in the presence of the RyR agonist ryanodine (at low concentrations) and blocked by the RyR antagonist ruthenium red. Additionally, neuropeptide release experiments show that these same RyR agonists and antagonists modulate Ca^{2+}-elicited neuropeptide release from permeabilized NHTs. Furthermore, amperometric recording of spontaneous release events from artificial transmitter-loaded terminals corroborated these ryanodine effects. Collectively, our findings suggest that RyR-dependent syntillas could represent mobilization of Ca^{2+} from vesicular stores. Such localized vesicular Ca^{2+} release events at the precise location of exocytosis could provide a Ca^{2+} amplification mechanism capable of modulating neuropeptide release physiologically.

The Journal of General Physiology

INTRODUCTION

Neuropeptide secretion is principally elicited by the influx of extracellular Ca^{2+} through voltage-gated channels. However, increasing evidence makes it clear that internal Ca^{2+} stores may provide another important source of Ca^{2+} affecting this process (Salzberg et al. 1997. The 51st Annual Meeting of the Society of General Physiologists. Abstr. 45; Collin et al., 2005; Berridge, 2006). Large dense core vesicles (LDCVs) or granules in several secretory systems, including neurohypophysial terminals (NHTs), contain a substantial amount of Ca^{2+} (Pozzan et al., 1994). In chromaffin cells, for instance, vesicular Ca^{2+} (Ca^{2+}_v) makes up 60% of the total Ca^{2+} contained in the cell (Haigh et al., 1989).

The precise role of Ca^{2+}_v is still quite controversial. The high buffering capacity of vesicles (Hutton, 1984) has led many to assume that Ca^{2+}_v is immobile and serves only as a means of removing Ca^{2+} from the cell (Nordmann and Zyzek, 1982; Pozzan et al., 1994). However, several studies suggest that Ca^{2+}_v can significantly regulate secretion (Nicaise et al., 1992; Thirion et al., 1995; Gerasimenko et al., 1996; Martinez et al., 1996; Scheenen et al., 1998; Mundorf et al., 2000; Mitchell et al., 2003; Mahapatra et al., 2004). For instance, in insulin-secreting β cells and chromaffin cells, depletion of Ca^{2+}_v markedly reduces secretion (Scheenen et al., 1998; Mundorf et al., 2000).

More recent studies have demonstrated that highly localized Ca^{2+} transients (Ca^{2+} syntillas) can be observed in isolated NHTs. These syntillas are ryanodine sensitive (De Crescenzo et al., 2004) and increase in frequency with depolarization (De Crescenzo et al., 2006). Our initial work has indicated that individual syntillas are incapable of eliciting spontaneous release events (McNally et al., 2009). However, these findings do not rule out a modulatory role for syntillas in evoked release or in other intracellular signaling pathways/processes.

The source of the Ca^{2+} released in these syntillas has yet to be ascertained. In LDCVs of NHTs, a large conductance

Correspondence to José R. Lemos: Jose.Lemos@umassmed.edu

J.M. McNally's present address is Dept. of Psychiatry, VA Boston Healthcare System, Harvard Medical School, Brockton, MA 02301.

S.D. Kraner's present address is Sanders Brown Center for Aging, University of Kentucky, Lexington, KY 40536.

Abbreviations used in this paper: AVP, arginine vasopressin; EM, electron microscopy; LDCV, large dense core vesicle; NH, neurohypophysis; NHT, neurohypophysial terminal; SV-2, synaptic vesicle protein 2.

The Rockefeller University Press $30.00
J. Gen. Physiol. Vol. 143 No. 6 693–702
www.jgp.org/cgi/doi/10.1085/jgp.201311110

nonspecific cation channel has been characterized that appears to be involved in secretion (Lee et al., 1992; Yin et al., 2002). Interestingly, this channel's properties are indistinguishable from the single-channel properties of mammalian RyRs (Coronado et al., 1994; Fill and Copello, 2002). However, it has not yet been determined if these channels are identical. Because Ca^{2+} syntillas in NHTs emanate from ryanodine-sensitive stores, localization of RyRs to the LDCV membrane would suggest that these granules are the origin of syntillas.

Here, we use immunogold labeling of NHTs to examine whether RyRs colocalize with LDCVs. Furthermore, we use single-channel analysis of the large conductance LDCV channel to establish if this channel is sensitive to pharmacological agents specific for RyR. Finally, RyR agonists and antagonists were also tested to determine if mobilization of this ryanodine-sensitive calcium store is capable of affecting hormone release from isolated NHTs. This diversified approach provides strong evidence that the LDCVs are involved in ryanodine-sensitive syntillas, which can modulate secretion of arginine vasopressin (AVP) from central nervous system terminals.

MATERIALS AND METHODS

Immuno–electron microscopy (EM) and Westerns

Freshly dissected mouse neurohypophyses (NHs) were fixed for 4 h at 4°C in 200 mM sodium cacodylate buffer containing 16 and 8%, respectively, purified monomeric paraformaldehyde and glutaraldehyde, pH 7.4, and then transferred directly into a 100-mM sodium cacodylate buffer, pH 7.4, to wash. The tissue was then quickly rinsed with ice-cold distilled water and transferred successively into cold (4°C) EtOH solutions for 10 min at each of four concentrations (50, 70, 80, and 90%), and then placed in a 2:1 mixture of EtOH and LR White Embedding Resin (Electron Microscopy Science) and allowed to incubate at room temperature for 30 min. The mixture was then replaced with pure LR White and allowed to stand for an additional hour, after which it was changed to fresh resin and left at 4°C overnight in a firmly sealed vial. The next morning, the tissue was embedded in gelatin capsules, overfilled, and cured at 58°C for ∼30 h.

For immunostaining, the fixed and embedded glands were cut into 80-nm-thick sections (Ultracut S microtome; Leica) and mounted on 200-mesh thin bar nickel grids. After drying, the grids were blocked for 1 h at room temperature with 1% ovalbumin and 0.2% cold water fish skin gelatin in PBS, pH 7.4, to prevent nonspecific binding. After blotting, the grids were incubated overnight at 4°C with a primary antibody found to be specific for type 2 RyR (Fig. 1 C) diluted in PBS, pH 7.4. After washing with Tris-buffered PBS, pH 7.4, for 20 min, the grids were incubated with 15–18-nm colloidal Au anti-rabbit for 1 h at room temperature, and then washed twice with Tris-buffered saline and once with distilled water. Finally, the labeled grids were stained briefly (3 min) in aqueous uranyl acetate solution, washed again with distilled water, and allowed to air dry. Labeled grids were observed in a microscope (JEOL100 CX; JEOL, Ltd.) for RyR type 2 (RyR_2)-specific antisera labeling.

Expression of RyR_2 in mouse NH and neurosecretosomes was monitored by immunoblotting using a specific rabbit antibody (see above). As both positive and negative controls for RyR, whole-cell lysates from mouse brain, skeletal muscle, and cardiac muscle were run alongside purified neurosecretosomes. Protein from purified NH and neurosecretosomes was resolved using a standard SDS/PAGE procedure (8% Tris-glycine precast gel, XCell mini cell; Invitrogen). Contents of the gel were then transferred to a nitrocellulose membrane (XCell blot module, constant 25 V for 2 h/overnight). The blot was then blocked for 1 h in PBS with 3% nonfat dried milk (PBS/M), and then incubated with necessary dilution of primary antibody in PBS/M for 1–2 h. The blot was then washed three times with PBS for 10 min before the addition of donkey anti–rabbit IgG horseradish peroxidase, or donkey anti–goat IgG horseradish peroxidase (1:5,000 in PBS/M, starting dilution). The blot was allowed to incubate in the secondary solution for 1 h, and then washed three times with PBS, as before. The blot was then developed with Super Signal West Dura (Thermo Fisher Scientific) for 5 min, after which the blot was read (ChemiDoc system; Bio-Rad Laboratories).

Immunohistochemistry

Male Sprague-Dawley rats (Taconic) weighing 200–250 g were sedated using CO_2 and immediately decapitated (Ortiz-Miranda et al., 2010). After removal of the anterior and intermediate lobes of the pituitary, the neural lobe was dissociated in a buffer at 37°C that contained (mM): 270 sucrose, 0.01 EGTA, and 10 HEPES-Tris, buffered at pH 7.3, 295–300 mOsm/L. The homogenate containing dissociated terminals was aliquoted equally into two 35-mm polypropylene glass-bottom micro-well dishes (MatTek Corporation) and washed initially with a low Ca^{2+} (3 µM of free Ca^{2+}) Locke's saline containing (mM): 140 NaCl, 5 KCl, 1.9 $CaCl_2$, 2 EGTA, 10 HEPES, 10 glucose, and 1.2 $MgCl_2$, pH 7.3, 295–300 mOsm/L, and slowly changed to a normal (2.2 mM $CaCl_2$ and no EGTA) Locke's saline to remove any floating debris. The tissue was fixed overnight in 4% paraformaldehyde phosphate buffer (PB) solution, pH 7, and washed three times in PB afterward. One dish was not exposed to primary antibodies and was used as a control for nonspecific binding. The other dish was exposed to a 1% Triton X-100 PB solution containing 10% donkey serum, an affinity-purified goat anti–neurophysin II (AVP) (2 µg/ml; Santa Cruz Biotechnology, Inc.), a rabbit polyclonal anti-RyR (2 µg/ml; Santa Cruz Biotechnology, Inc.), and a mouse monoclonal anti–synaptic vesicle protein 2 (SV-2; Developmental Studies Hybridoma Bank, National Institute of Child Health and Human Development-University of Iowa). All dishes were incubated overnight, washed with PB, and exposed to fluorescently tagged secondary antibodies (Molecular Probes) for 3–5 h at room temperature to visualize each labeled protein. The mixture of secondary antibodies included Alexa Fluor 350 donkey anti–goat IgG, Alexa Fluor 488 donkey anti–mouse IgG, Alexa Fluor donkey anti–rabbit IgG, and 10% donkey serum in a 1% Triton X-100 PB solution. After a final series of washes, the dishes were mounted with Prolong (Molecular Probes) and sealed with a glass coverslip to increase the fluorescence life of the secondary antibodies. Images were obtained with an inverted microscope (Axiovert 200M; Carl Zeiss) interfaced with a camera (AxioCam MRm; Carl Zeiss) fitted to a 63-X Plan/Apochromat oil-immersion lens, with a numerical aperture of 1.4. Axiovert 40 software (V.4.6.3.0; Carl Zeiss) was used for acquisition and image analysis. Images of one or more terminals were obtained in stacks at every 0.27 µm along the length of the terminals. The length was set as the point where the fluorescence signal was no longer visible from both the top and bottom ends of terminals. Images were deconvoluted using a high stringency fast iterative algorithm and corrected for fluorescence cross-talk between stacks. Fluorescence levels in control dishes were at or below nonspecific levels for all three wavelengths (not depicted).

The amount of antigen labeling associated within each isolated terminal was estimated from the pan RyR (RyR_{pan}), SV-2, and AVP immunofluorescence signals within a single dish. Experiments

were replicated three times. Terminals that did not label for AVP were assumed to contain oxytocin (see Custer et al., 2007).

Colocalization analysis of the RyR_{pan} and SV-2/AVP fluorescence signals was done using JACoP under ImageJ software. Pearson's coefficients were obtained for each terminal using an intensity correlation coefficient-based approach, and mean ± SEM was calculated (Bolte and Cordelières, 2006). This analysis provides a reliable and accurate calculation of the localization of individual signals, pixel by pixel, within a region of interest (in our case, an individual terminal). Higher values of Pearson's coefficients denote a greater level of signal colocalization (Bolte and Cordelières, 2006).

Isolation of bovine LDCVs

The LDCVs of bovine NHs were obtained as reported previously (McNally et al., 2004). Cows were used here because they give much more (>200 times) material than rats or mice, which is necessary to isolate and purify the LDCVs. In brief, bovine pituitaries were collected at a local slaughterhouse and then rapidly transferred into warm (37°C) isosmotic homogenizing solution (HS): 300 mM sucrose, 10 mM Tris-HEPES, and 1 mM EGTA, pH 7.0. After transporting the glands back to the laboratory, they were rinsed with HS and the NH was carefully dissected out. The NH was briefly immersed in Listerine, rinsed with fresh HS, and then homogenized in ice-cold HS. The resulting homogenate was sequentially centrifuged, and then LDCVs were separated on a Percoll (GE Healthcare) density gradient, yielding an extremely pure preparation of LDCVs. Purified LDCVs were aliquoted and rapidly frozen at −80°C for later use.

Single-channel analysis in planar lipid bilayer

Bilayers were formed as described previously (Yin et al., 2002; McNally et al., 2004). In brief, phosphatidylethanolamine and phosphatidylserine (10 mg/ml in chloroform; Avanti Polar Lipids, Inc.) were mixed at a 3:1 ratio (wt/wt), and then dried under a stream of argon. The lipids were resuspended in decane (Sigma-Aldrich) and used for formation of bilayers on a 150–250-µm aperture in a polystyrene cup (Sarstedt). The aperture was positioned between the two chambers of the bilayer apparatus filled with 50 mM KCl, 10 mM HEPES, and 2 mM EGTA, pH 7.3 (1 ml trans and 0.7 ml cis). After bilayer formation, a 250:150-mM KCl gradient (*cis/trans*) was established across the bilayer. 10 µM of free Ca^{2+} was added to the cis chamber, which corresponded to the cytoplasmic side of the channel. The trans chamber remained at zero Ca^{2+} (2 mM EGTA) to ensure proper channel orientation. Purified bovine LDCVs were then added to the cis chamber with stirring, after which the current across the bilayer was monitored using a standard patch-clamp amplifier (EPC9; HEKA). After channel incorporation was observed, chamber stirring was stopped to avoid further channel incorporation. Channel activity data were then collected at 20 kHz and stored in a computer and analyzed with a single-channel analysis program (TAC X4.1; Bruxton). For histogram fits, data were digitally filtered at 400 Hz and sorted in bins of ∼1/3 pA. For control and treated datasets, three normal distributions were fit to the data according to least-squares criteria. The standard deviations varied from 0.8 to 1.8 pA. Although data contained evidence for a fourth conductance state (open state 3), the probability was low enough that fitting the data with an additional normal distribution did not improve the fit. Therefore, all data were fit assuming two open and one closed state. Open times for each conductance state are reported as means ± 95% confidence limits (*t* test).

Permeabilized terminal release assay

NHTs were isolated from male Sprague-Dawley CD rats (150–250 g) as described by Cazalis et al. (1987a). The dissociated terminals were equally loaded onto filters (0.45 µm; Acrodisc; Gelman Scientific) and perfused with normal Locke's saline for 45 min at a flow rate of 50 µl per minute. The NHTs were then perfused at 100 µl per minute with a potassium glutamate solution (Cazalis et al., 1987b) containing 0.05–1 µM of free calcium, which was determined using the WEBMAXC Standard program. After a 1-h perfusion with the potassium glutamate solution, the NHTs were permeabilized with 1 µM digitonin alone or in the presence of agonist (≤3 µM) or antagonist (≥10 µM) concentrations of ryanodine or ruthenium red (5 µM). Perfusate was collected in 4-min fractions before, during, and after digitonin application. The samples were then frozen at −20°C until assayed for AVP using a specific enzyme-linked immunoassay (Assay Designs) with a sensitivity of 0.25 pg per well (Custer et al., 2007). All samples from each experiment were run in a single assay with an inter-assay coefficient of variation of 5%.

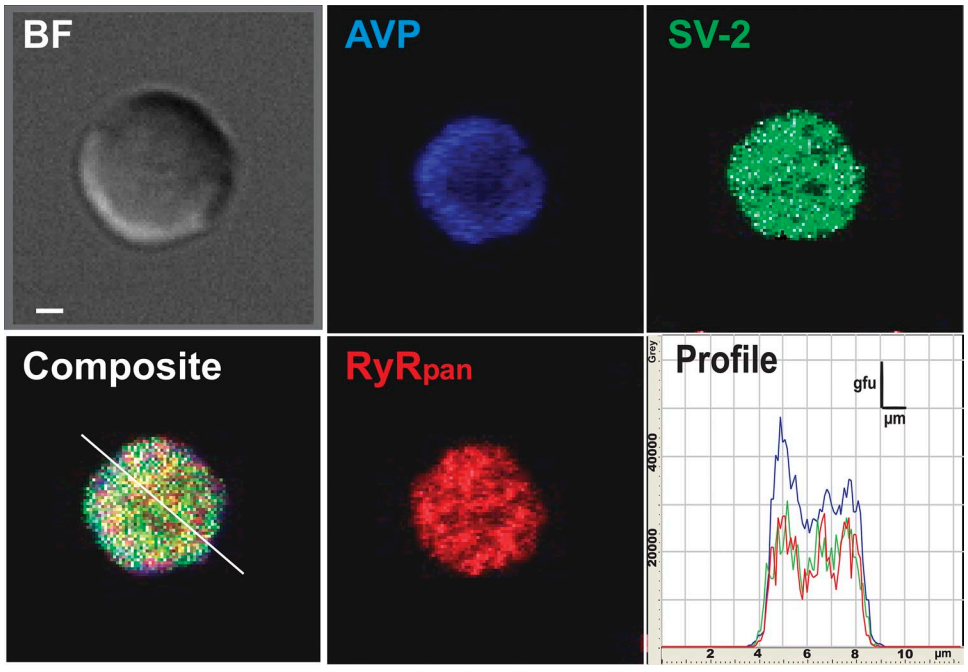

Figure 1. Immunolabeling of RyRs in NHTs. Immunocytochemical localization of RyRs (red), LDCV marker AVP (blue), and synaptic vesicle marker SV-2 (green) in an individual isolated NHT (BF, bright field). Images were obtained at 0.27-µm increments along the length of the terminal, deconvoluted using a high stringency fast iterative algorithm, and corrected for fluorescence cross talk. Only the middle stack is shown. Signal profile (bottom right) was generated at the plane shown by the white line in the composite image (bottom left). Note that all signals show a similar intensity pattern. Terminal size is shown in the profile graph. Bars: 10,000 grey fluorescent units; 1 µm.

Amperometry and false transmitter loading

Loading NHTs with the false transmitter dopamine (DA) was accomplished through the inclusion of 15 mM DA in the pipette solutions used. NHTs were patched in the whole-cell configuration and voltage clamped at a holding potential of −80 mV. DA was allowed to dialyze into the NHT, where it could then be trafficked into acidic compartments, including the LDCVs (Kim et al., 2000). This process generally required 5 min for sufficient loading. While loading, a 5-µm diameter carbon fiber electrode, voltage clamped at 700 mV, was placed in close apposition to the plasma membrane of the terminal. When loaded LDCVs undergo exocytosis, DA released from NHTs contacts the carbon fiber, where its subsequent oxidation results in a detectable current flow through the electrode. Successful loading was determined by the appearance of spontaneous amperometric events at a resting membrane potential of −80 mV (see Fig. 6). See also McNally et al. (2009).

Statistical analysis

Data are given as means ± SEM. Statistical analysis of the effects of experimental agents on fluorescence, channel activity, and neuropeptide release was performed using a either a Student's *t* test or one-way ANOVA, followed by a Dunnett's test to determine significant differences between means (Sigma Stat; Jandel Scientific). Statistical significance for all analyses was established as $P < 0.05$.

Source of chemicals

All chemicals used in these studies were obtained from either Sigma-Aldrich (ruthenium red), Ascent Scientific (ryanodine), or as indicated in the text.

RESULTS

Localization of RyRs via immunofluorescence and immunogold EM

Mouse NHTs have been shown to possess all three subtypes of the RyR (De Crescenzo et al., 2004, 2006). If RyRs are localized to the membranes of LDCVs, their terminal distribution should be similar to other proteins known to be present at the membranes of synaptic vesicles. Thus, we co-labeled mouse NHTs with antibodies capable of recognizing all three isoforms of the RyR (Okkenhaug et al., 2006; Divangahi et al., 2009), the neuropeptide AVP (Ortiz-Miranda et al., 2010), and the well-known LDCV marker SV-2 (Buckley and Kelly, 1985; Feany et al., 1992). The immunofluorescence signals for AVP, RyR, and SV-2 all appeared similar (Fig. 1, bottom left). This overall similarity was corroborated via analysis of the distribution profiles of each signal (Fig. 1, bottom right). Pearson's coefficients were estimated from individual terminals to quantify the level of colocalization

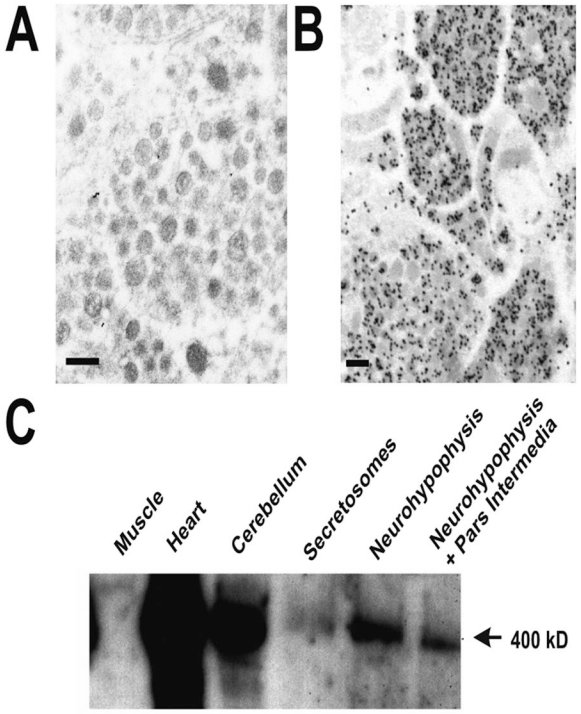

Figure 2. Immunogold labeling of neurosecretory granules is specific, and RyR_2 is present in the NH. (A) Control, without primary RyR_2 antibody but using normal rabbit IgG, and labeled with 15 nm colloidal gold secondary antibody. No nonspecific gold labeling is observed. (B) Immunogold labeling of LDCVs using an antibody to AVP (PS45), conjugated to 18 nm colloidal gold. Gold labeling of AVP is apparent. Bars, 500 nm. (C) Western blot showing specificity of the RyR_2 antibody. Lanes 1–6 contained equal amounts of homogenate from mouse muscle, heart, cerebellum, NHT, NH, and NH plus pars intermedia, respectively. As expected, no RyR_2 labeling is seen in the lane loaded with skeletal muscle homogenate, whereas the lanes loaded with heart and cerebellar homogenate show strong labeling. RyR_2 labeling was observed in both the lanes containing neurohypophysial homogenate and NHT (secretosome) homogenate. This indicates that RyR_2 was present in NHTs.

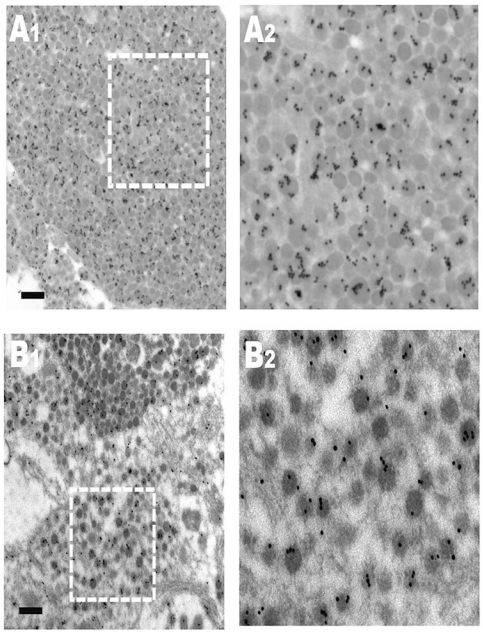

Figure 3. RyR_2 labeling is localized specifically to neurosecretory granules. (A and B) Representative electron micrographs of neurohypophysial slices labeled with immunogold beads conjugated to RyR_2-specific primary antibody. (A_1 and B_1) 18- and 16-nm, respectively, immunogold labeling. A_2 and B_2 show magnified views of the areas delineated by the dotted squares in A_1 and B_1.

between RyR and either the AVP- or SV-2–dependent immunofluorescence. When the AVP- and RyR-dependent signals were compared, a Pearson's coefficient colocalization value of 0.81 ± 0.02 (n = 20) was obtained. For the SV-2 versus RyR signals, the Pearson's coefficient value was 0.80 ± 0.03. These coefficients show a strong level of signal colocalization.

To corroborate the immunofluorescence results, EM was coupled with immunogold labeling to provide a higher resolution means of visually localizing RyR to the LDCV. Fixed neurohypophysial slices from different animals (n = 5) were labeled with primary antisera confirmed to be specific for type 2 RyR (Fig. 2 C). Antibody labeling was visualized by conjugating the secondary antibody to immunogold beads (15–18 nm). Electron micrographs of labeled slices (Fig. 3, A and B) show that immunogold bead labeling was specifically localized to LDCVs. The granules (density = 20/μm^2) showed a significant (t test; P = 0.04) 3.4-fold increase in labeling compared with the control area density (5.8/μm^2). Furthermore, bead labeling in NHTs but outside of LDCVs (3.1/μm^2) with no IgG (see Fig. 2 A) controls (2.7 gold particles/μm^2) were even lower, and secondary IgGs alone showed no labeling (not depicted). From the averages, 69.8 ± 7.5% of LDCVs demonstrate immunoreactivity for RyR_2, which is comparable (t test; P = 0.34) to mitochondria (79 ± 4%) but not to micro-vesicles (10%). To show LDCV specificity, we labeled slices with AVP antibody (Fig. 2 B). As expected, these showed an even higher density (>250/μm^2) of labeling in LDCVs.

RyR agonists/antagonists affect LDCV channel activity

Previously, we have identified and characterized a large multi-conductance nonspecific cation channel that is bimodally regulated by Ca^{2+}, which resides in the LDCV membrane (Lee et al., 1992; Yin et al., 2002). The characteristics of this LDCV channel are remarkably similar to those of the mammalian RyR (Coronado et al., 1994; Fill and Copello, 2002), suggesting that these two channels may be the same. Therefore, the LDCV channel was tested to determine if it had the same characteristic response as the RyR to its agonists and antagonists.

After initially assessing the basal activity level of these channels (Fig. 4 A, top), 10 μM ryanodine, a specific

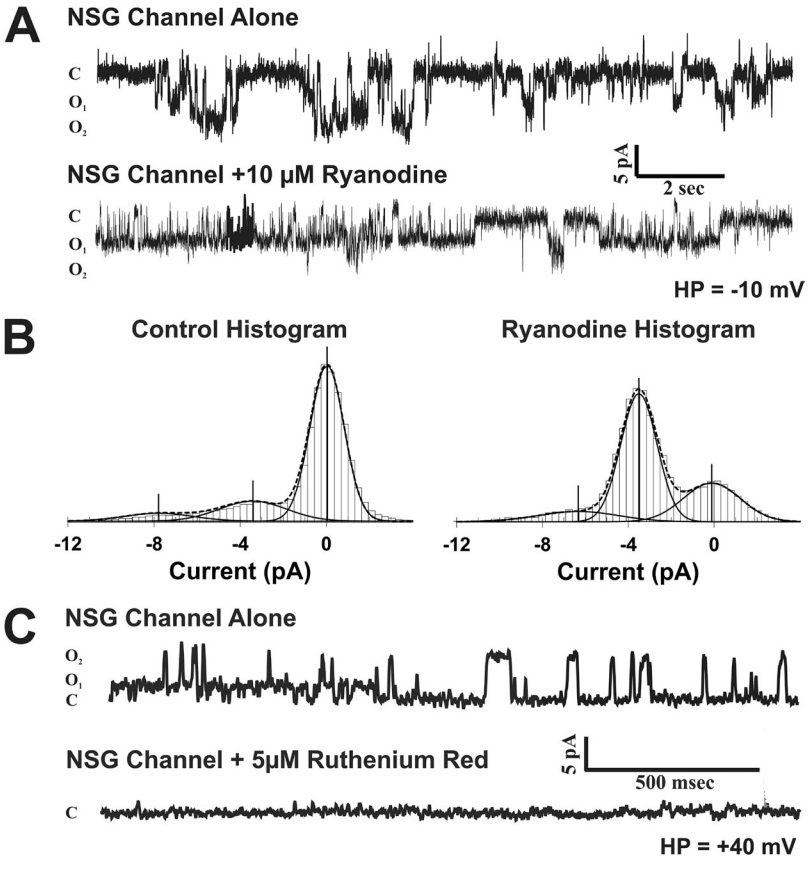

Figure 4. LDCV channel responds to agonist concentrations of ryanodine and the RyR antagonist ruthenium red in the same characteristic manner as RyRs. (A) Single-channel recordings showing the effect of the RyR agonist ryanodine on the LDCV channel isolated in a phosphatidylethanolamine/phosphatidylserine (3:1) planar lipid bilayer. The bilayer apparatus contained 250 mM KCl, 10 mM HEPES, and 10 μM of free Ca^{2+} in the cis well and 150 mM KCl and 10 mM HEPES in the trans well. (Top) A large conductance cation channel, isolated from purified LDCVs, was recorded at a steady holding potential of −10 mV for several minutes. (Bottom) After the addition of 10 μM ryanodine to the cis well, the activity of the same channel was recorded. (B) All-points amplitude histogram for the channel alone (right, control) and the same channel after the addition of ryanodine (left). Ryanodine caused an increase in the channel's open probability at a decreased conductance. Under control conditions, the LDCV channel remained in the closed state (C) 74% of the time and was in a lower open (O_1) state (−3.4 pA) 18.5% or a higher open (O_2) state (−7.8 pA) 7.5% of the time. After the application of ryanodine, the channel remained in the closed state only 29% of the time, and it was in a lower open state (−3.5 pA) 60.5% or a higher open state (6.3 pA) only 10.5% of the time. Thus, the addition of ryanodine caused a significant (P < 0.05) change in open probability for both the main conductance state and the subconductance state of the LDCV channels. (C) Representative single-channel recording showing the effects of ruthenium red on the LDCV channel. Here, the bilayer apparatus contained 150 mM KCl, 10 mM HEPES, and 10 μM of free Ca^{2+} in the cis well and 150 mM KCl and 10 mM HEPES in the trans well. (Top) An LDCV channel isolated in a planar bilayer was recorded at a holding potential of +40 mV for several minutes. Under control conditions, the LDCV channel remained in the closed state (C) 57% of the time and was in open state one (O_1) 36% and open state two (O_2) 7% of the time. (Bottom) After the addition of the RyR antagonist ruthenium red (5 μM), the channel was rapidly inhibited and remained in the closed state for the duration of the recording.

agonist of the RyR, was added to the cis well (Fig. 4 A, bottom). Ryanodine application led to a substantial increase (see Fig. 4 legend) in the probability of the channel residing in its subconductance state ($n = 3$; see Fig. 4 B). This change in probability was caused by a significant ($P < 0.05$) change in the lifetimes of each conductance state after ryanodine addition. The lifetime of the subconductance state increased >2.5-fold (from 12.0 ± 0.9 to 31.7 ± 2.0 msec), and that of the main open state decreased to 41% of control (from 29 ± 6 to 12 ± 2 msec). The lifetime of the closed state also decreased (from 69 ± 7 to 22 ± 4 msec) significantly ($P < 0.05$). We note that to maximize the likelihood of channel incorporation into the bilayer, the free Ca^{2+} concentration was maintained at 10 μM in the cis chamber of the bilayer apparatus. This Ca^{2+} concentration has been shown previously to elicit peak activity for both the LDCV channels (Lee et al., 1992) and RyR (Coronado et al., 1994). Thus, the measured lifetimes were determined at a Ca^{2+} concentration that increases channel activity.

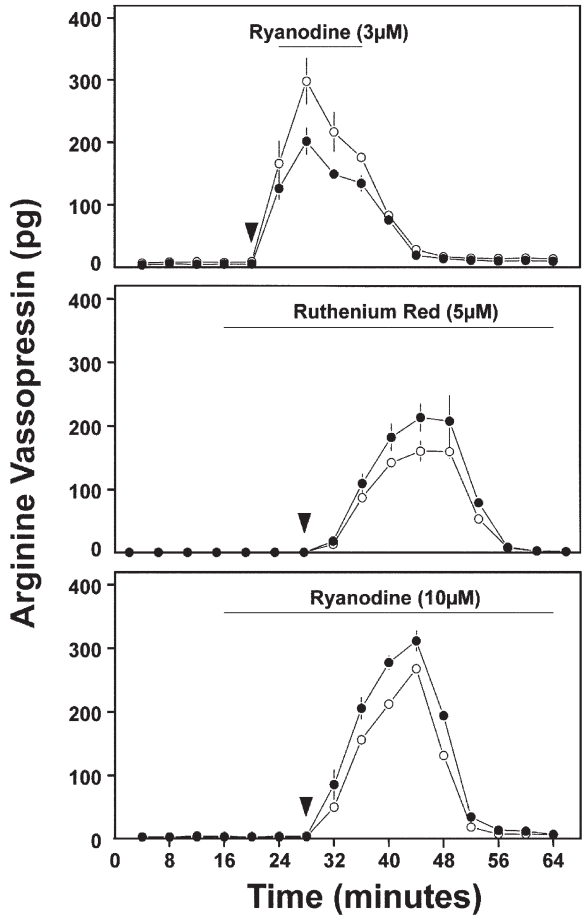

Figure 5. Effect of ryanodine and ruthenium red on calcium-induced AVP release from permeabilized NHTs. The NHTs were perfused with potassium glutamate buffer containing 200 nM to 1 μM of free calcium and permeabilized with 1 μM digitonin (arrow) for 16 min. (Top) An agonist concentration (3 μM) of ryanodine (○; $n = 3$) applied (solid line) during the digitonin permeabilization potentiated significantly ($P < 0.05$) the calcium-induced AVP release compared with digitonin alone (●; $n = 3$). (Middle) Treatment with 5 μM ruthenium red (○; $n = 3$; solid line), an RyR antagonist, before and during the digitonin permeabilization decreased significantly ($P < 0.05$) the calcium-induced AVP release compared with digitonin alone (●; $n = 3$). (Bottom) An antagonist concentration (10 μM) of ryanodine (○; $n = 3$) applied (solid line) during the digitonin permeabilization significantly reduced ($P < 0.05$) the calcium-induced AVP release compared with digitonin alone (●; $n = 3$). All values are expressed as the mean ± SEM. The perfusion rate is the same for all three graphs, 100 μl/min. The free calcium concentration is 1 μM for the top and middle graphs, and 200 nM for the bottom graph.

The effects of the RyR antagonist ruthenium red on LDCV channels was also examined using the same protocol as described above. After the addition of 5 μM ruthenium red to the cis chamber, there was a significant ($P < 0.05$) reduction in the p_o from 0.59 ± 0.09 under basal conditions to 0.08 ± 0.04 with ruthenium red ($n = 3$). This effect is shown in Fig. 4 C, where the activity of this LDCV channel ceases several minutes after the application of ruthenium red.

RyR agonists/antagonists modulate secretion

Previous work has suggested that the LDCV channel described above is involved in neuropeptide secretion (Lee et al., 1992). Given these findings, we wanted to determine whether or not mobilization of Ca^{2+} from ryanodine-sensitive LDCVs could play a role in neuropeptide secretion from NHTs. Therefore, we examined the effects of agonists/antagonists of the RyR on hormone release from a population of isolated NHTs. For these experiments, NHTs were permeabilized with 1 μM digitonin while being perfused with a solution containing 1 μM of free Ca^{2+} buffered with 2 mM EGTA to give the half-maximal $[Ca^{2+}]_i$ for evoked peptide hormone release (Lee et al., 1992). The addition of an agonist concentration of ryanodine (3 μM) to the perfusate resulted in a 37% increase in Ca-evoked AVP release (Fig. 5, top), whereas the addition of a higher concentration of ryanodine (10 μM) caused a 25% reduction in 200 nM of Ca-evoked AVP release (Fig. 5, bottom). Furthermore, the addition of the RyR antagonist ruthenium red (5 μM) was able to inhibit the Ca^{2+}-evoked AVP release by 24% (Fig. 5, middle).

Additionally, amperometric recording of spontaneous release events from artificial transmitter-loaded terminals corroborated these ryanodine effects (Fig. 6). Agonist levels of ryanodine (5 μM) elicited a significant ($P < 0.05$) increase in the rate of spontaneous release, a 2.42 ± 0.45–fold increase compared with the rate under basal conditions ($n = 5$ terminals), although higher antagonist levels of ryanodine (500 μM) were observed to significantly ($P < 0.05$) decrease spontaneous release to 0.31 ± 0.1 times the basal rate ($n = 7$ terminals). To rule out any vehicle effect on the release rate, normal Locke's solution alone was added to the bath in the same manner that antagonist ryanodine was added. This vehicle

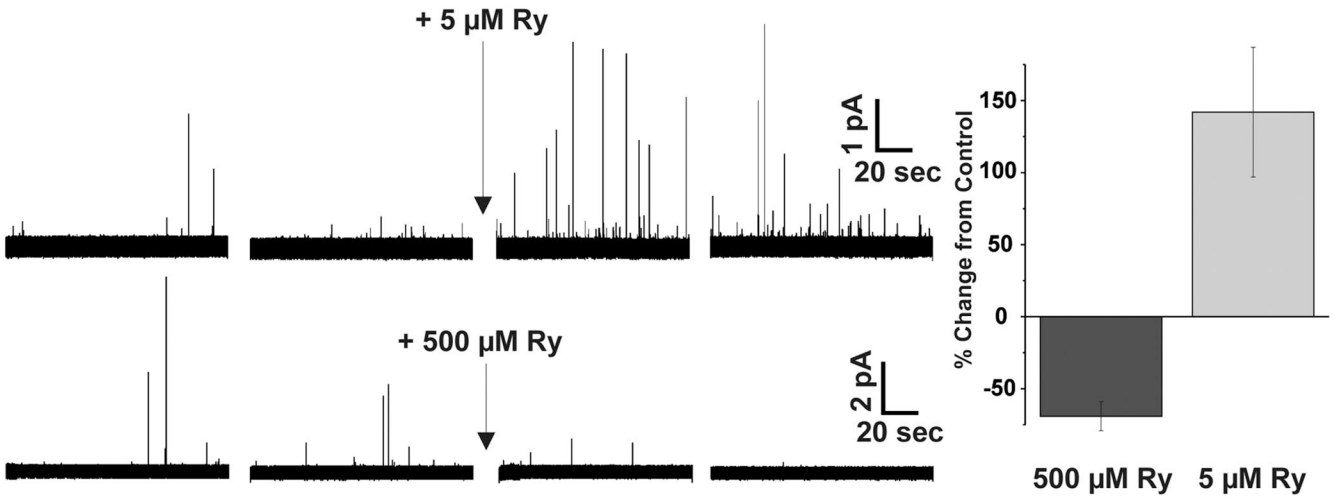

Figure 6. Ryanodine affects the basal rate of exocytotic activity from nerve terminals as measured by amperometry. Amperometric traces provide an example of the effects of ryanodine on spontaneous exocytotic release. Each trace represents sequential 2-min amperometric records from false transmitter–loaded terminals perforated-patched with β-escin, and held at a resting membrane potential of −80 mV in normal Locke's solution. (Top) The addition of RyR agonist levels of ryanodine (5 µM) results in an increase in the basal release rate. (Bottom) Conversely, the addition of ryanodine at an RyR antagonistic concentration (500 µM) to the bath between the second and third amperometric trace results in a reduction of the basal release rate. (Right) Bar graph summarizing the effects of ryanodine on release across terminals.

treatment appeared to slightly but not significantly ($P > 0.05$) raise the spontaneous release rate 1.4-fold ($n = 3$); thus, we may be underestimating the effect of antagonist ryanodine on basal release.

DISCUSSION

The results presented here provide several lines of evidence supporting the hypothesis that LDCVs possess a dynamic ryanodine-sensitive store of Ca^{2+}, which possibly represents the source of Ca^{2+} syntillas. First, immunohistochemistry (Fig. 1) and EM findings (Figs. 2 and 3) show that the RyR is localized specifically to LDCVs in NHTs. Second, a large multi-conductance cation channel, with biophysical and pharmacological characteristics similar to the RyR, was isolated from the membranes of LDCVs (Lee et al., 1992; Yin et al., 2002) and is now shown to be affected by specific RyR agonists and antagonists (Fig. 4), suggesting that RyR and LDCV channels are one and the same. Finally, we present hormone release results (Figs. 5 and 6) indicating that ryanodine-sensitive Ca^{2+} stores can modulate secretion from NHTs.

Our earlier work suggested that the LDCV cation channel is "synaptophysin-like" because of the effects that the synaptophysin-specific SY-38 antibody had on channel activity (Yin et al., 2002). However, more recent studies characterizing the channel activity of purified synaptophysin (Gincel and Shoshan-Barmatz, 2002) describe a channel with properties that are markedly different from the LDCV channel. Interestingly, this discrepancy could be because the C-terminal region of synaptophysin, the site of SY-38 antibody binding, exhibits significant homology with a region of the RyR thought to contain one of the calcium-binding domains (Coronado et al., 1994). This might also explain the effects that the SY-38 antibody had on the calcium dependence of the LDCV channel (Yin et al., 2002). However, additional experimentation is required to determine the validity of this hypothesis.

As demonstrated by literature in the field, RyR pharmacology is quite complex (Sutko et al., 1997; Fill and Copello, 2002). This fact has led to inconsistencies in the concentrations of ryanodine used as an agonist versus as an antagonist in published work. Here, we observed that 10 µM ryanodine acted as an agonist in our single-channel studies. At present, we have not studied the effects of ryanodine at different concentrations on LDCV channel properties. However, our findings are largely consistent with previous RyR single-channel studies using similar ryanodine concentrations (Buck et al., 1992). Most importantly, statistical analyses performed for the lifetime of both the main and the subconductance states of the LDCV channels (Fig. 4) showed a significant change in both after the addition of ryanodine, which is characteristic of RyRs. Interestingly, this same ryanodine concentration when used in our permeabilized terminal assay of hormone secretion yielded antagonist-like results. Such disparities in the effects of ryanodine are likely caused by differences in experimental conditions, particularly the concentration of free Ca^{2+}, which plays an essential role in modulating the interaction of ryanodine with RyR.

Previous studies from our group and others provide strong evidence that the isolated LDCV preparations used in this work are quite pure (Lemos et al., 1991; Lee

et al., 1992; Yin et al., 2002). However, we have not been able to completely rule out contamination of these preparations with other intracellular organelles, which potentially contain the large conductance channels studied here. Further, our hormone-secretion findings cannot conclusively establish the precise localization of RyR. Taking all of these factors into account, we nevertheless remain confident that channels isolated in our experiments are in fact localized to neurohypophysial LDCVs for several reasons. First, there is little evidence for the presence of endoplasmic reticulum in NHTs. Second, our earlier studies have shown that mitochondrial poisoning agents have no effect on Ca^{2+} syntillas, providing evidence that functional mitochondrial RyRs are not present in this preparation (De Crescenzo et al., 2004). These findings suggest that these two established sources of RyR-mediated intracellular Ca^{2+} release are not present in NHTs, leaving LDCVs as the most likely source. We cannot, however, rule out a different localization and/or function for these channels/receptors, and this could affect the interpretation of our results.

The data described in this study suggest that Ca^{2+} release from ryanodine-sensitive intracellular stores, identified as the LDCVs, may facilitate neuropeptide secretion. Ryanodine-sensitive intracellular Ca^{2+} release has been shown to facilitate transmitter release in several different neuronal systems (Llano et al., 2000; Bardo et al., 2002; Galante and Marty, 2003; Conti et al., 2004; Ouyang et al., 2005), leading to speculation that syntillas may function in precisely this manner in NHTs (Berridge, 2006; Oheim et al., 2006). In contrast, such Ca^{2+} release has been found to play little or no role in transmitter release in other systems (Carter et al., 2002; Lim et al., 2003). Recently, in the NH, ryanodine-sensitive calcium release has been credited with playing a physiologically relevant role in oxytocin secretion (Jin et al., 2007). Mobilization of these Ca^{2+} stores results in an increase in basal release. How exactly release is facilitated still remains to be elucidated.

Our previous work in both NHTs and chromaffin cells has shown that release of Ca^{2+} from such stores is not sufficient to directly elicit spontaneous exocytosis (ZhuGe et al., 2006; McNally et al., 2009). However, these findings looked only at individual Ca^{2+} syntillas and do not rule out a modulatory role of RyR-sensitive calcium release on either evoked release or vesicle-trafficking mechanisms. The proximity of docked LDCVs to voltage-gated Ca^{2+} channels could enable them to act as an elegant Ca^{2+} amplifier if external Ca^{2+} entry alone is insufficient to affect LDCV exocytosis (Salzberg et al. 1997. The 51st Annual Meeting of the Society of General Physiologists. Abstr. 45). Beyond a direct interaction with the Ca^{2+}-sensing mechanism involved in secretion, Ca^{2+} has also been shown to regulate several other intracellular processes (Berridge, 2006). There is precedence to suggest such a role for intracellular calcium release in the hypothalamic neurohypophysial system. Ludwig and Leng (2006) have shown that intracellular calcium from IP_3 receptors has a priming effect on dendritic neuropeptide secretion from magnocellular neurons. This priming involves the relocation of secretory granules from reserve pools to the readily releasable pool. It is possible that intracellular calcium release could play a similar role in vesicle mobility and in the recruitment of vesicles to docked pools on the plasma membrane at NHTs.

In conclusion, our work suggests that voltage-dependent Ca^{2+} transients may reflect release from ryanodine-sensitive vesicular stores. The increases in intracellular Ca^{2+} that occur in these terminals may play a role in modulating peptide hormone secretion by either a Ca^{2+}-induced Ca^{2+} release mechanism or by activation of RyRs via depolarization. Such a process could play a major role in the control of neuropeptide release from NHTs.

This study was supported by National Institutes of Health grants (NS24978 and NS063192 to J.R. Lemos and NS40966 to B.M. Salzberg), a University of Massachusetts Medical School grant to S. Ortiz-Miranda, and a National Research Service Award (NS048628) fellowship to J.M. McNally.

The authors declare no competing financial interests.

Sharona E. Gordon served as editor.

Submitted: 26 September 2013
Accepted: 1 May 2014

REFERENCES

Bardo, S., B. Robertson, and G.J. Stephens. 2002. Presynaptic internal Ca^{2+} stores contribute to inhibitory neurotransmitter release onto mouse cerebellar Purkinje cells. *Br. J. Pharmacol.* 137:529–537. http://dx.doi.org/10.1038/sj.bjp.0704901

Berridge, M.J. 2006. Calcium microdomains: Organization and function. *Cell Calcium.* 40:405–412. http://dx.doi.org/10.1016/j.ceca.2006.09.002

Bolte, S., and F.P. Cordelières. 2006. A guided tour into subcellular colocalization analysis in light microscopy. *J. Microsc.* 224:213–232.

Buck, E., I. Zimanyi, J.J. Abramson, and I.N. Pessah. 1992. Ryanodine stabilizes multiple conformational states of the skeletal muscle calcium release channel. *J. Biol. Chem.* 267:23560–23567.

Buckley, K., and R.B. Kelly. 1985. Identification of a transmembrane glycoprotein specific for secretory vesicles of neural and endocrine cells. *J. Cell Biol.* 100:1284–1294.

Carter, A.G., K.E. Vogt, K.A. Foster, and W.G. Regehr. 2002. Assessing the role of calcium-induced calcium release in short-term presynaptic plasticity at excitatory central synapses. *J. Neurosci.* 22:21–28.

Cazalis, M., G. Dayanithi, and J.J. Nordmann. 1987a. Hormone release from isolated nerve endings of the rat neurohypophysis. *J. Physiol.* 390:55–70.

Cazalis, M., G. Dayanithi, and J.J. Nordmann. 1987b. Requirements for hormone release from permeabilized nerve endings isolated from the rat neurohypophysis. *J. Physiol.* 390:71–91.

Collin, T., A. Marty, and I. Llano. 2005. Presynaptic calcium stores and synaptic transmission. *Curr. Opin. Neurobiol.* 15:275–281. http://dx.doi.org/10.1016/j.conb.2005.05.003

Conti, R., Y.P. Tan, and I. Llano. 2004. Action potential-evoked and ryanodine-sensitive spontaneous Ca^{2+} transients at the presynaptic terminal of a developing CNS inhibitory synapse. *J. Neurosci.* 24:6946–6957. http://dx.doi.org/10.1523/JNEUROSCI.1397-04.2004

Coronado, R., J. Morrissette, M. Sukhareva, and D.M. Vaughan. 1994. Structure and function of ryanodine receptors. *Am. J. Physiol.* 266:C1485–C1504.

Custer, E.E., S.I. Ortiz-Miranda, T. Knott, R. Rawson, C. Elvey, R.H. Lee, and J.R. Lemos. 2007. Identification of the neuropeptide content of individual rat neurohypophysial terminals. *J. Neurosci. Methods*. 163:226–234.

De Crescenzo, V., R. ZhuGe, C. Velázquez-Marrero, L.M. Lifshitz, E. Custer, J. Carmichael, F.A. Lai, R.A. Tuft, K.E. Fogarty, J.R. Lemos, and J.V. Walsh Jr. 2004. Ca^{2+} syntillas, miniature Ca^{2+} release events in terminals of hypothalamic neurons, are increased in frequency by depolarization in the absence of Ca^{2+} influx. *J. Neurosci.* 24:1226–1235. http://dx.doi.org/10.1523/JNEUROSCI.4286-03.2004

De Crescenzo, V., K.E. Fogarty, R. Zhuge, R.A. Tuft, L.M. Lifshitz, J. Carmichael, K.D. Bellvé, S.P. Baker, S. Zissimopoulos, F.A. Lai, et al. 2006. Dihydropyridine receptors and type 1 ryanodine receptors constitute the molecular machinery for voltage-induced Ca^{2+} release in nerve terminals. *J. Neurosci.* 26:7565–7574. http://dx.doi.org/10.1523/JNEUROSCI.1512-06.2006

Divangahi, M., H. Balghi, G. Danialou, A.S. Comtois, A. Demoule, S. Ernest, C. Haston, R. Robert, J.W. Hanrahan, D. Radzioch, and B.J. Petrof. 2009. Lack of CFTR in skeletal muscle predisposes to muscle wasting and diaphragm muscle pump failure in cystic fibrosis mice. *PLoS Genet*. 5:e1000586.

Feany, M.F., S. Lee, R.H. Edwards, and K.M. Buckley. 1992. The synaptic vesicle protein SV2 is a novel type of transmembrane transporter. *Cell*. 70:861–867.

Fill, M., and J.A. Copello. 2002. Ryanodine receptor calcium release channels. *Physiol. Rev*. 82:893–922.

Galante, M., and A. Marty. 2003. Presynaptic ryanodine-sensitive calcium stores contribute to evoked neurotransmitter release at the basket cell-Purkinje cell synapse. *J. Neurosci.* 23:11229–11234.

Gerasimenko, O.V., J.V. Gerasimenko, P.V. Belan, and O.H. Petersen. 1996. Inositol trisphosphate and cyclic ADP-ribose-mediated release of Ca^{2+} from single isolated pancreatic zymogen granules. *Cell*. 84:473–480. http://dx.doi.org/10.1016/S0092-8674(00)81292-1

Gincel, D., and V. Shoshan-Barmatz. 2002. The synaptic vesicle protein synaptophysin: Purification and characterization of its channel activity. *Biophys. J.* 83:3223–3229. http://dx.doi.org/10.1016/S0006-3495(02)75324-1

Haigh, J.R., R. Parris, and J.H. Phillips. 1989. Free concentrations of sodium, potassium and calcium in chromaffin granules. *Biochem. J.* 259:485–491.

Hutton, J.C. 1984. Secretory granules. *Experientia*. 40:1091–1098. http://dx.doi.org/10.1007/BF01971456

Jin, D., H.X. Liu, H. Hirai, T. Torashima, T. Nagai, O. Lopatina, N.A. Shnayder, K. Yamada, M. Noda, T. Seike, et al. 2007. CD38 is critical for social behaviour by regulating oxytocin secretion. *Nature*. 446:41–45. http://dx.doi.org/10.1038/nature05526

Kim, K.T., D.S. Koh, and B. Hille. 2000. Loading of oxidizable transmitters into secretory vesicles permits carbon-fiber amperometry. *J. Neurosci.* 20:RC101.

Lee, C.J., G. Dayanithi, J.J. Nordmann, and J.R. Lemos. 1992. Possible role during exocytosis of a Ca^{2+}-activated channel in neurohypophysial granules. *Neuron*. 8:335–342. http://dx.doi.org/10.1016/0896-6273(92)90299-S

Lemos, J.R., C.J. Lee, K.A. Ocorr, G. Dayanithi, and J.J. Nordmann. 1991. Possible role for neurosecretory granule channel that resembles gap junctions. *Ann. NY Acad. Sci.* 635:480–482. http://dx.doi.org/10.1111/j.1749-6632.1991.tb36533.x

Lim, R., S. Oleskevich, A.P. Few, R.N. Leao, and B. Walmsley. 2003. Glycinergic mIPSCs in mouse and rat brainstem auditory nuclei: modulation by ruthenium red and the role of calcium stores. *J. Physiol.* 546:691–699. http://dx.doi.org/10.1113/jphysiol.2002.035071

Llano, I., J. González, C. Caputo, F.A. Lai, L.M. Blayney, Y.P. Tan, and A. Marty. 2000. Presynaptic calcium stores underlie large-amplitude miniature IPSCs and spontaneous calcium transients. *Nat. Neurosci.* 3:1256–1265. http://dx.doi.org/10.1038/81781

Ludwig, M., and G. Leng. 2006. Dendritic peptide release and peptide-dependent behaviours. *Nat. Rev. Neurosci.* 7:126–136. http://dx.doi.org/10.1038/nrn1845

Mahapatra, N.R., M. Mahata, P.P. Hazra, P.M. McDonough, D.T. O'Connor, and S.K. Mahata. 2004. A dynamic pool of calcium in catecholamine storage vesicles. Exploration in living cells by a novel vesicle-targeted chromogranin A-aequorin chimeric photoprotein. *J. Biol. Chem.* 279:51107–51121. http://dx.doi.org/10.1074/jbc.M408742200

Martinez, J.R., S. Willis, S. Puente, J. Wells, R. Helmke, and G.H. Zhang. 1996. Evidence for a Ca^{2+} pool associated with secretory granules in rat submandibular acinar cells. *Biochem. J.* 320:627–634.

McNally, J.M., D.J. Woodbury, and J.R. Lemos. 2004. Syntaxin 1A drives fusion of large dense-core neurosecretory granules into a planar lipid bilayer. *Cell Biochem. Biophys.* 41:11–24. http://dx.doi.org/10.1385/CBB:41:1:011

McNally, J.M., V. De Crescenzo, K.E. Fogarty, J.V. Walsh, and J.R. Lemos. 2009. Individual calcium syntillas do not trigger spontaneous exocytosis from nerve terminals of the neurohypophysis. *J. Neurosci.* 29:14120–14126. http://dx.doi.org/10.1523/JNEUROSCI.1726-09.2009

Mitchell, K.J., F.A. Lai, and G.A. Rutter. 2003. Ryanodine receptor type I and nicotinic acid adenine dinucleotide phosphate receptors mediate Ca^{2+} release from insulin-containing vesicles in living pancreatic beta-cells (MIN6). *J. Biol. Chem.* 278:11057–11064. http://dx.doi.org/10.1074/jbc.M210257200

Mundorf, M.L., K.P. Troyer, S.E. Hochstetler, J.A. Near, and R.M. Wightman. 2000. Vesicular Ca^{2+} participates in the catalysis of exocytosis. *J. Biol. Chem.* 275:9136–9142. http://dx.doi.org/10.1074/jbc.275.13.9136

Nicaise, G., K. Maggio, S. Thirion, M. Horoyan, and E. Keicher. 1992. The calcium loading of secretory granules. A possible key event in stimulus-secretion coupling. *Biol. Cell.* 75:89–99. http://dx.doi.org/10.1016/0248-4900(92)90128-N

Nordmann, J.J., and E. Zyzek. 1982. Calcium efflux from the rat neurohypophysis. *J. Physiol.* 325:281–299.

Oheim, M., F. Kirchhoff, and W. Stühmer. 2006. Calcium microdomains in regulated exocytosis. *Cell Calcium.* 40:423–439. http://dx.doi.org/10.1016/j.ceca.2006.08.007

Okkenhaug, H., K.H. Weylandt, D. Carmena, D.J. Wells, C.F. Higgins, and A. Sardini. 2006. The human ClC-4 protein, a member of the CLC chloride channel/transporter family, is localized to the endoplasmic reticulum by its N-terminus. *FASEB J.* 20:2390–2392.

Ortiz-Miranda, S., G. Dayanithi, C. Velazquez-Marrero, S.N. Treistman, and J.R. Lemos. 2010. Differential modulation of N-type calcium channels by micro-opioid receptors in oxytocinergic versus vasopressinergic neurohypophysial terminals. *J. Cell. Physiol.* 255:276–288.

Ouyang, K., H. Zheng, X. Qin, C. Zhang, D. Yang, X. Wang, C. Wu, Z. Zhou, and H. Cheng. 2005. Ca^{2+} sparks and secretion in dorsal root ganglion neurons. *Proc. Natl. Acad. Sci. USA*. 102:12259–12264. http://dx.doi.org/10.1073/pnas.0408494102

Pozzan, T., R. Rizzuto, P. Volpe, and J. Meldolesi. 1994. Molecular and cellular physiology of intracellular calcium stores. *Physiol. Rev.* 74:595–636.

Scheenen, W.J., C.B. Wollheim, T. Pozzan, and C. Fasolato. 1998. Ca^{2+} depletion from granules inhibits exocytosis. A study with insulin-secreting cells. *J. Biol. Chem.* 273:19002–19008. http://dx.doi.org/10.1074/jbc.273.30.19002

Sutko, J.L., J.A. Airey, W. Welch, and L. Ruest. 1997. The pharmacology of ryanodine and related compounds. *Pharmacol. Rev.* 49:53–98.

Thirion, S., E.L. Stuenkel, and G. Nicaise. 1995. Calcium loading of secretory granules in stimulated neurohypophysial nerve endings. *Neuroscience.* 64:125–137. http://dx.doi.org/10.1016/0306-4522(94)00414-Z

Yin, Y., G. Dayanithi, and J.R. Lemos. 2002. Ca^{2+}-regulated, neurosecretory granule channel involved in release from neurohypophysial terminals. *J. Physiol.* 539:409–418. http://dx.doi.org/10.1113/jphysiol.2001.012943

ZhuGe, R., V. DeCrescenzo, V. Sorrentino, F.A. Lai, R.A. Tuft, L.M. Lifshitz, J.R. Lemos, C. Smith, K.E. Fogarty, and J.V. Walsh Jr. 2006. Syntillas release Ca^{2+} at a site different from the microdomain where exocytosis occurs in mouse chromaffin cells. *Biophys. J.* 90:2027–2037. http://dx.doi.org/10.1529/biophysj.105.071654